Positron Studies of Defects 2011

In-situ hydrogen sorption 2D-ACAR facility for the study of metal hydrides for hydrogen storage

W.J. Legerstee[a*], J. de Roode[a], A. Anastasopol[a], C.V. Falub[b], S.W.H. Eijt[a]

[a]Department of Radiation, Radionuclides & Reactors, Delft University of Technology, Mekelweg 15, NL-2629 JB Delft, The Netherlands
[b]Solid State Physics Laboratory, Swiss Federal Institute of Technology ETH-Zürich, Schafmattstrasse 16, CH-8093 Zürich, Switzerland

Abstract

We developed a dedicated hydrogen sorption setup coupled to a positron 2D-ACAR (two-dimensional Angular Correlation of Annihilation Radiation) setup employing a ^{22}Na-source, which will enable to collect 2D-ACAR momentum distributions *in-situ* as a function of temperature, hydrogen pressure and hydrogen content. In parallel, a dedicated glovebox was constructed for handling air-sensitive metal and metal hydride samples, with a special entrance for the 2D-ACAR sample insert. The 2D-ACAR setup was tested in first measurements on a $Pd_{0.75}Ag_{0.25}$ foil and on a ball-milled MgH_2 powder in both the hydrogen loaded and desorbed states. The hydrogen loaded $Pd_{0.75}Ag_{0.25}H_x$ sample was kept under a 1 bar hydrogen pressure to prevent partial desorption during measurements at room temperature. The collected 2D-ACAR distributions of $Pd_{0.75}Ag_{0.25}$ and $Pd_{0.75}Ag_{0.25}H_x$ showed similar features as observed in previous studies. The broadening of the ACAR distributions observed for the Mg to MgH_2 metal-insulator transition was compared in a quantitative manner to ab-initio calculations reported in the literature.

1. Introduction

Metal hydrides are promising materials for the storage of hydrogen as a sustainable energy source for the development of fuel cell cars [1]. Magnesium hydride (MgH_2) is a promising cheap and abundant hydrogen storage material, with a high gravimetric storage capacity of up to 7.6 wt%. However, the uptake and discharge of hydrogen proceeds slowly and at low hydrogen equilibrium pressures for practical operation temperatures below ~100 °C. These properties can be improved by turning to nanoscale MgH_2 grain sizes [2]. Vacancy-related defects play an important role in the mobility of hydrogen in metal hydrides, which is a crucial factor to achieve sufficiently fast hydrogen sorption kinetics. Recent positron Doppler broadening and positron lifetime studies monitored the

---

* Corresponding author. Tel.: +31-15-278 1344; fax: +31-15-278 6422.
E-mail address: w.j.legerstee@tudelft.nl.

evolution of vacancies and small vacancy clusters in MgH_2 [3-6], $Pd_{1-y}Ag_yH_x$ [7] and $NaAlH_4$ [8] metal hydrides in measurements as a function of hydrogen cycling. The metal-to-metal-hydride transition is often accompanied by large changes in the electronic structure, in particular when the metal hydride is an insulator, such as MgH_2 [9]. These large changes in the electronic structure have a pronounced effect on their optical properties, leading to promising applications of metal hydrides in fast optical-switching hydrogen sensors [10]. As discussed in [9], the electron momentum distribution of MgH_2 is correspondingly expected to broaden significantly relative to that of the Mg metal phase, as should be observable in 2D-ACAR distributions.

In order to enable *in-situ* collection of 2D-ACAR distributions as a function of temperature, hydrogen content and pressure, we developed a dedicated hydrogen sorption setup coupled to the Delft positron 2D-ACAR setup employing a ^{22}Na-source. The airtight sample holder insert further enables 2D-ACAR studies on air-sensitive samples in general. To this aim, we further employ a new dedicated glovebox with a special entrance for the 2D-ACAR sample insert. Here, we describe the instrumental details of the *in-situ* hydrogen sorption 2D-ACAR facility and first results obtained on a $Pd_{0.75}Ag_{0.25}$ foil and a ball-milled MgH_2 powder in the metal and metal hydride phases, demonstrating its potential for the study of metal hydrides for hydrogen storage and hydrogen sensors.

2. In-situ 2D-ACAR setup and dedicated glovebox

Figure 1a shows the central part of the 2D-ACAR setup at the Reactor Institute Delft (RID) destined for measurements of bulk samples with thicknesses in the (sub-)mm range [11]. It consists of an electromagnet, a lead container with the positron source and a vacuum chamber, all mounted on a supporting table. The 2.7×10^8 Bq (strength in June 2011) ^{22}Na positron source is mounted on a rod which can move into the bore of one of the poles of a water-cooled electromagnet. The uniform magnetic field generated by the electromagnet is used to guide the positrons with a maximum kinetic energy of 540 keV towards the sample. The spot size of the positron beam on the sample depends on the strength of the magnetic field, which can be changed with the current through the electromagnet and the gap between the poles. In the present setup the distance between the poles of the iron yoke is 60 mm (Figure 1b). In this configuration a current of 16.5 A through the electromagnet generates a magnetic field of 0.71 T. This yields a spot size on the sample of ~8 mm.
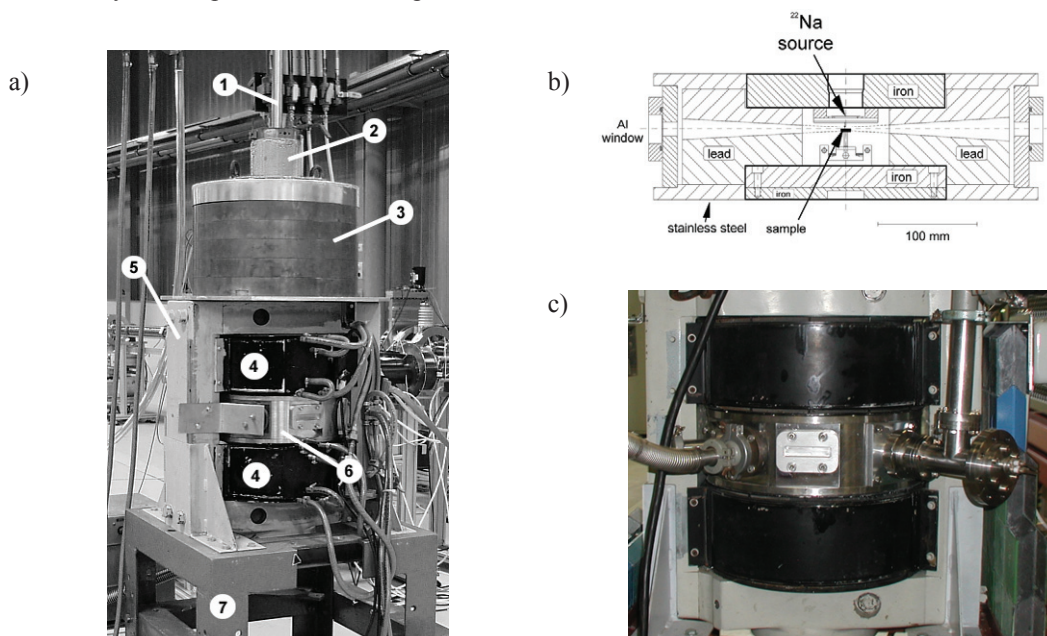

Figure 1 a) Overview of the ^{22}Na-source based 2D-ACAR vacuum chamber. 1 – rod holding the ^{22}Na positron source, 2 – source lead container, 3 – additional lead shielding, 4 – electromagnet coils, 5 – iron yoke, 6 – vacuum chamber, 7 – supporting table;
b) Cross-sectional view of the ^{22}Na-source based 2D-ACAR vacuum chamber (without inserted load-lock sample holder);
c) ^{22}Na-source based 2D-ACAR vacuum chamber with inserted load-lock sample holder (right) for *in-situ* hydrogen sorption studies.

The vacuum chamber is placed between the poles of the electromagnet. The sample is placed inside a vacuum chamber with a pressure of about 5×10^{-2} mbar in order to avoid annihilations of positrons with air molecules. The two position sensitive γ ray detectors are of the Anger camera type [12] purchased from AuRa Scientific. These detectors each consist of a single NaI(Tl) crystal with a hexagonal shape and a thickness of 9.6 mm and associated electronics. The 61 photomultipliers are optically coupled to the glass window of the crystal in a honeycomb structure. A 27 mm thick lead ring shields the edge of the crystal, leaving a circular effective area with a diameter of 0.418 m. A gamma ray photon with an energy of about 511 keV, hitting the NaI crystal, will generate scintillation photons detected by several photomultiplier tubes. Subsequently, the signals from the photomultipliers are pre-amplified, combined and fed into summing resistor networks, which generate position information (horizontal and vertical) with respect to the detector and information on the energy of the gamma ray photon. Only events with an energy 511 ± 75 keV will be processed. The analogue position signals from both detectors are fed into a data-acquisition unit. Additional trigger pulses generated by the detectors are used to set the time coincidence window for the annihilation events. A coincidence window of 100 ns is used [13]. Furthermore, the signals are digitized and sent to a personal computer. The software combines the digitized signals and increases a counter at the appropriate position in a two-dimensional array of 256 × 256 channels. The angle corresponding to a channel depends on the detector-detector distance (e.g. one channel corresponds to 0.2 mrad for a 23.245 m detector-detector distance). The overall resolution is $(1.4\cdot 10^{-3}\ m_oc) \times (1.4 \cdot10^{-3}\ m_oc)$ [13] (with m_o the electronic rest mass and *c* the velocity of light in vacuum) after Gaussian broadening of the measured 2D-ACAR distributions in the direction perpendicular to the plane of the sample, in order to account for the finite spot size of the positron beam on the sample.

A dedicated load-lock sample holder system was designed to enable 2D-ACAR studies on air-sensitive samples and to load and unload hydrogen storage materials in the 2D-ACAR setup, which will enable *in-situ* 2D-ACAR measurements as a function of hydrogen cycling. Figure 2a presents a schematic drawing of the load-lock sample holder system for *in-situ* 2D-ACAR studies and 2D-ACAR studies of air-sensitive samples. The RVS load-lock tube system (Figure 2a and 2b) creates a separate sample space which can be filled with hydrogen gas at pressures of up to 1 bar (at least) relative to the vacuum maintained in the 2D-ACAR chamber.
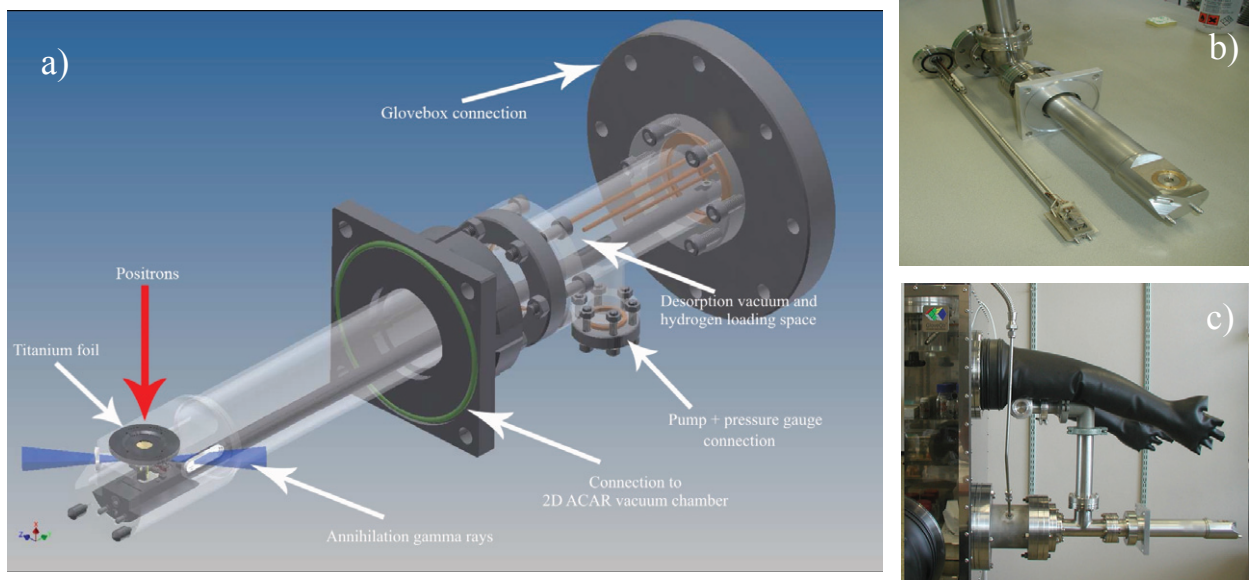

Figure 2. a) Schematic drawing of the load-lock sample system which can be attached to the 2D-ACAR vacuum chamber for *in-situ* hydrogen sorption 2D-ACAR measurements, and to the dedicated GloveQb glovebox for handling of air-sensitive samples. b) Sample support rod (left) and outer part of the load-lock sample holder system (right); c) Ar-filled load-lock system (bottom right) attached to the dedicated GloveQb glovebox (left).

A 13.5 μm thin Ti-foil forms the 8 mm diameter entrance port for the positron beam to the sample space inside the load-lock system and is fixed using a brass ring and glued to the RVS load-lock tube. The integrity of the Ti-foil has been tested up to pressure differences of 2 bar against vacuum and 1 bar against ambient pressure. Further, the load-lock system can be evacuated down to a pressure of 2×10^{-6} mbar. The sample can be heated from room temperature up to a temperature of 500 ^{o}C. Therefore, *in-situ* 2D-ACAR measurements can be performed under conditions relevant for many promising metal hydride hydrogen storage materials such as Mg-based and NaAlH$_4$-based metal hydrides. During hydrogen desorption, the pressure of the desorbing hydrogen gas in the load-lock system is monitored by a pressure gauge (MKS baratron 627BX.1MDD1B) sensitive in the pressure range above 0.1 mbar. Temperature is monitored by a chromel/alumel thermocouple (type K) attached to the sample. Two types of sample supports can be applied, a cup with lateral dimensions of 12.5×7.6 mm^2 and a depth of 2 mm for 2D-ACAR measurements on powders, and a plate with lateral dimensions of 13×8 mm^2 for measurements on foils and single crystals. Foils are fixed on the sample support using clamps at the edges of the foil, while powders supplied to the cup are gently pressed and the surface flattened using a glass plate during preparation in the dedicated glovebox. The height of the sample surface can be adjusted such that it is well-aligned with the middle of the 0.2 mm thin aluminium exit windows for the annihilation gamma rays and with the centre of both Anger cameras for proper collection of 2D-ACAR distributions.

A dedicated, customer adapted glovebox system was purchased from GloveQb [14], and is used for the supply of the air-sensitive samples to the load-lock sample holder in an inert Ar gas environment, with O$_2$ and H$_2$O concentrations below 1 ppm. After the sample support with the mounted sample is fixed at the correct height on the rod of the load-lock sample holder (see Fig. 2b, left) inside the glovebox, it can be moved into the Ar-filled load-lock sample tube system (Fig. 2b, right) attached to the glovebox at a dedicated glovebox entrance (see Figure 2c). Subsequently, the complete Ar-filled airtight insert can be detached from the glovebox and moved to the 2D-ACAR setup for *in-situ* 2D-ACAR measurements under controlled gas conditions. The dedicated glovebox was further fitted with a second dedicated entrance on the top for transfer of samples to an Anton Paar XRD sample container with heating stage for complementary *in-situ* hydrogen sorption XRD measurements. The GloveQb glovebox can further be used for the preparation of air-sensitive samples (such as most metal hydrides for hydrogen storage) and transfer to other sample analysis equipment, including a sensitive hydrogen thermal desorption spectroscopy (TDS) setup and SEM. The weight of samples can be determined using a Mettler Toledo MS205DU weighing balance positioned inside the glovebox.

3. 2D-ACAR study of MgH$_2$ and Pd$_{0.75}$Ag$_{0.25}$H$_x$

Here we report initial tests of the *in-situ* 2D-ACAR setup on two types of sample, namely a) a 80 μm thin Pd$_{0.75}$Ag$_{0.25}$ foil (Alfa Aesar) and b) a 0.12 g ball-milled MgH$_2$ powder (Sigma Aldrich). The Pd-Ag foil had lateral dimensions of 13.5×8 mm^2. 2D-ACAR distributions with 11×10^6 and 8×10^6 coincidence counts, respectively, were collected, with an evacuated sample space inside the load-lock system during the measurements on the Pd-Ag foil, while a 1 bar H$_2$ back pressure was used in order to prevent desorption during the measurements on the Pd-Ag-H foil. The foil was hydrogen loaded using a hydrogen pressure of 6 bar, heating the foil first to 573 K for a four hour activation treatment, and subsequently temperature was reduced in steps of 100 K down to room temperature, keeping temperature fixed for one hour at each step to facilitate hydrogen absorption. This procedure leads to a hydrogen fraction absorbed in Pd$_{0.75}$Ag$_{0.25}$H$_x$ foils of typically $x \sim 0.2$-0.4. In these test experiments, the hydrogen loading was still performed *ex-situ*, in the sensitive hydrogen thermal desorption setup HYDRA [15]. The presence of the additional 13.5 μm Ti-foil as entrance to the sample space and the 0.2 mm thin Al windows caused a reduction of 40% of the coincidence count rate, as could be expected. 2D-ACAR distributions of the ball-milled MgH$_2$ powder were collected before and after hydrogen desorption at 623 K for 20 hours using the HYDRA setup (the base pressure is 10^{-5} mbar), which ensures that all the hydrogen was desorbed from the sample. 2D-ACAR distributions with 32×10^6 and 19×10^6 coincidence counts, respectively, were collected using a 1 bar Ar pressure in the load-lock system in both cases. We determined that the contribution of possible annihilation of positrons in the Ar-gas was negligible, i.e. below the false coincidence count rate of ~0.025 c/s. We further checked that the emptied sample holder cup does not contribute to the 2D-ACAR distribution either. The collected 2D-ACAR distributions were normalized to the total number of coincidence counts and processed using the ACAR2D MatLab program [16].
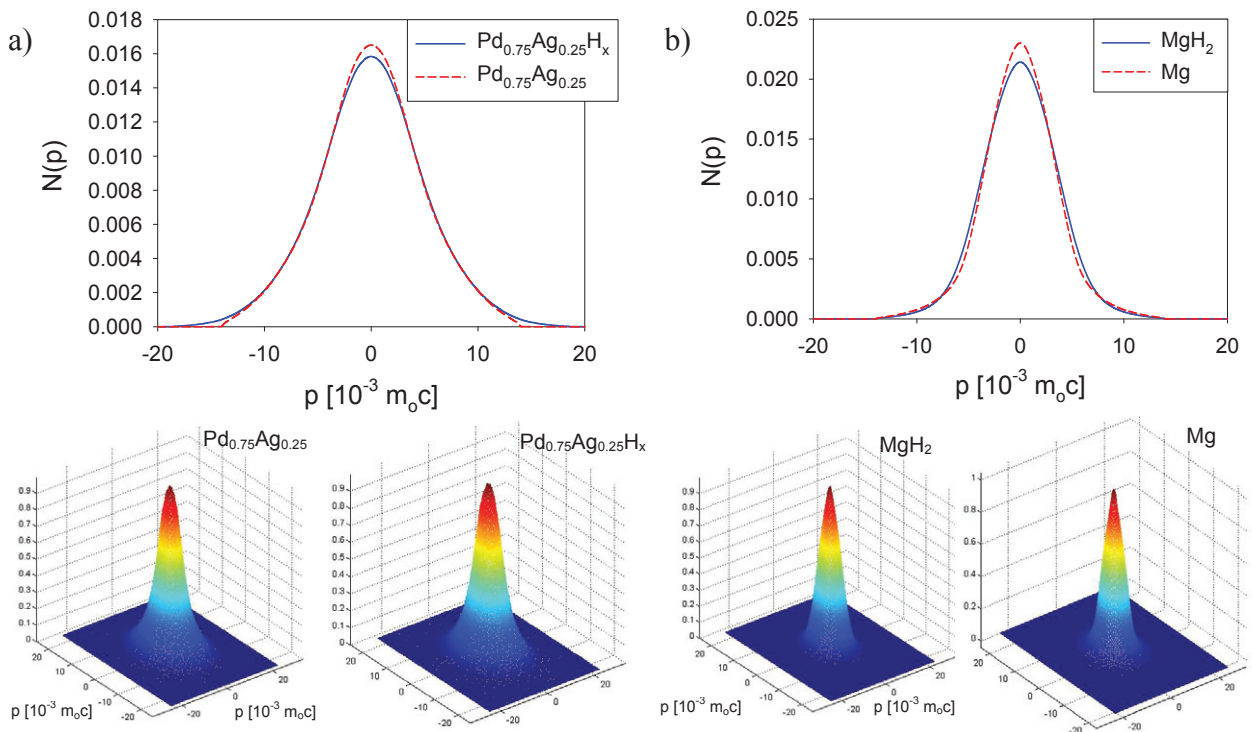
Figure 3. a) 1D-ACAR distributions of a Pd-Ag foil before and after the *ex-situ* hydrogen loading; b) 1D-ACAR distributions of ball-milled MgH$_2$ and (desorbed) Mg powders. The corresponding 2D-ACAR distributions are presented below.

Figure 3a shows the room-temperature 1D-ACAR distributions of the Pd-Ag foil before and after the *ex-situ* hydrogen loading, extracted from the corresponding 2D-ACAR distributions using the ACAR2D program. Clearly, the 1D-ACAR distribution of the Pd-Ag foil is narrower at low momenta compared to the hydrogen loaded Pd-Ag-H foil. This trend is consistent with previous ACAR measurements on Pd and PdH$_{0.72}$ single crystals by Hasegawa *et al*. [17]. Both 1D-ACAR distributions show relatively broad wings with significant intensity in the range up to at least ~15·10^{-3} $m_o c$ similar to reported in [17], resulting from the contributions of Pd(4d) valence electron states.

The 1D-ACAR distributions collected on the ball-milled MgH$_2$ and Mg powders (Fig. 3b) do not show such broad wings, as could be expected for s-p valence electron systems. The Mg-to-MgH$_2$ metal-insulator transition leads to a clear broadening by +11% of the 1D-ACAR momentum distributions with extracted widths at FWHM of 7.4·10^{-3} $m_o c$ and 8.2·10^{-3} $m_o c$, respectively. This is caused by the change in electronic structure between Mg metal, which shows a nearly-free-electron like behaviour with a Fermi momentum of p_F~5.4 ·10^{-3} $m_o c$ [18], and MgH$_2$, which is an insulator with localized electron orbitals primarily associated to hydrogen atoms [19] leading to a clear broadening in momentum space [9, 20]. The observed broadening is about half the size of the theoretical broadening by +21% deduced from ab-initio calculations of the Compton profiles of Mg [18, 9] and MgH$_2$ [20, 9], in which we took the contribution of the experimental resolution into account. The difference is mainly caused by the presence of defects in the ball-milled powders. Further, it could also be affected by the influence of the positron wave function on the electron-positron momentum distribution. Similar widths of 7.5·10^{-3} $m_o c$ and 8.8·10^{-3} $m_o c$ were observed for 1D-ACAR distributions of Pd-capped Mg$_{0.7}$Ti$_{0.3}$ and Mg$_{0.7}$Ti$_{0.3}$H$_2$ thin films, respectively, collected at 3 keV using the reactor-based intense low energy POSH beam as the positron source (see e.g. [13]). The reduction in intensity of the 1D-ACAR distribution at p=0 is in line with positron Doppler studies of Mg and MgH$_2$ thin films, which revealed a clear reduction in the Doppler S-parameter upon transition from the metal to insulator phase [21, 4, 6, 9].

4. Conclusion

The Delft positron 2D-ACAR facility was extended to enable *in-situ* studies as a function of hydrogen cycling of bulk metal hydride samples. A special insert was developed for the application of controlled gas environments in the 2D-ACAR sample chamber, in particular for *in-situ* loading of hydrogen storage materials, and will enable one to perform 2D-ACAR measurements as a function of hydrogen sorption. In combination with a dedicated new glovebox, this opens up the general possibility to handle air-sensitive samples for 2D-ACAR studies. 2D-ACAR distributions collected in first test experiments on *ex-situ* loaded $Pd_{0.75}Ag_{0.25}(H_x)$ foils and ball-milled MgH_2 and Mg powders yield results consistent with previous ACAR and Doppler broadening studies. A clear broadening of the electron-positron momentum distribution is observed for the Mg-to-MgH_2 metal-insulator transition. The change in FWHM is half the size expected from ab-initio calculations, primarily due to the abundant presence of open-volume defects, most likely surfaces and grain boundaries, in the ball-milled powders. The *in-situ* hydrogen sorption 2D-ACAR setup can be applied to a wide variety of metal hydrides, both for hydrogen storage applications where key properties of vacancy-related defects can be examined – important for the hydrogen sorption kinetics – as well as for the development of advanced fast optical-switching hydrogen sensors, owing to the sensitivity of the 2D-ACAR method for electronic structure properties of the metal/metal hydride as the key functional element of such sensors.

Acknowledgements

References

[1] L. Schlapbach, A. Züttel, Nature 414 (2001) 353.
[2] A. Zaluska, L. Zaluski, J.O. Strom-Olsen, J. Alloys Compds. 288 (1999) 217.
[3] H. Leegwater, H. Schut, W. Egger, A. Baldi, B. Dam, and S.W.H. Eijt, Appl. Phys. Lett. 96 (2010) 121902.
[4] R. Checchetto, N. Bazzanella, A. Miotello, R.S. Brusa, A. Zecca, A. Mengucci, J. Appl. Phys. 95 (2004) 1989.
[5] R. Checchetto, N. Bazzanella, A. Kale, A. Miotello, S. Mariazzi, R.S. Brusa, P. Mengucci, C. Macchi, A. Somoza, W. Egger, and L. Ravelli, Phys. Rev. B 84 (2011) 054115.
[6] S.W.H. Eijt, H. Leegwater, H. Schut, A. Anastasopol, W. Egger, L. Ravelli, C. Hugenschmidt, B. Dam, J. Alloys Compds. 509S (2011) S567.
[7] K. Sakaki, R. Date, M. Mizuno, H. Araki, Y. Shirai, Acta Mater. 54 (2006) 4641.
[8] K. Sakaki, Y. Nakamura, E. Akiba, M.T. Kuba, C.M. Jensen, J. Phys. Chem. C 114 (2010) 6869.
[9] S.W.H. Eijt, Phys. Stat. Solidi (c) 6 (2009) 2561.
[10] M. Slaman, B. Dam, H. Schreuders, R. Griessen, Int. J. Hydrogen Energy 33 (2008) 1084.
[11] C.V. Falub, PhD thesis, Delft University of Technology (Delft University Press, Delft, 2002).
[12] H.O. Anger, Rev. Sci. Instr. 29 (1958) 27.
[13] C.V. Falub, P.E. Mijnarends, S.W.H. Eijt, M.A. van Huis, A. van Veen, H. Schut, Phys. Rev. B 66 (2002) 075426.
[14] http://www.gloveqb.com/
[15] D.E. Nanu, W.J. Legerstee, S.W.H. Eijt, W.G. Haije, J.F. Vente, M.G. Tucker, A.J. Böttger, Acta Mater. 56 (2008) 6132.
[16] L. Chai, MSc thesis, Delft University of Technology (2010).
[17] M. Hasegawa, H. Asano, M. Hirabayashi, in *Positron Annihilation −Proceedings of the sixth International Conference on Positron Annihilation*, P.G. Coleman, S.C. Sharma, L.M. Diana (Eds.), (North Holland, Amsterdam, 1982) p. 234-236.
[18] M. Brancewicz, H. Reniewicz, A. Andrejczuk, L. Dobrzyński, E. Żukowski, S. Kaprzyk, Solid State Phen. 112 (2006) 123.
[19] R. Yu and P.K. Lam, Phys. Rev. B 37 (1988) 8730.
[20] J. Felsteiner, M. Heilper, I. Gertner, A.C. Tanner, R. Opher, K.-F. Berggren, Phys. Rev. B 23 (1981) 5156.
[21] S.W.H. Eijt, R. Kind, S. Singh, H. Schut, W.J. Legerstee, R.W.A. Hendrikx, V.L. Svetchnikov, R.J. Westerwaal, B. Dam, J. Appl. Phys. 105 (2009) 043514.